# Electronic Structure of $TlBa_2CaCu_2O_{7-\delta}$

R. P. Vasquez
Center for Space Microelectronics Technology
Jet Propulsion Laboratory, California Institute of Technology
Pasadena, California 91109-8099

D. L. Novikov and A. J. Freeman
Science and Technology Center for Superconductivity
Department of Physics and Astronomy, Northwestern [University
Evanston, Illinois 60208-3112

M. P. Siegal
Sandia National Laboratories
Albuquerque, New Mexico 8718 S-1421

## Abstract

The core levels of $TlBa_2CaCu_2O_{7-\delta}$ (Tl-1212) epitaxial films have been measured with x-ray photoelectron spectroscopy (XPS). The valence electronic structure has been determined using the full- potential linear muffin tin orbital band structure method and measured with XPS. The calculations show that a van Hove singularity (vHs) lies above the Fermi level ($E_F$) for the stoichiometric compound ($\delta=0$), while for 50% oxygen vacancies in the Tl-O layer ($\delta=0.5$) $E_F$ is in close proximity to the vHs. Samples annealed in nitrogen (to reduce the hole overdoping by the removal of oxygen) exhibit higher core level binding energies and higher $T_c$, consistent with a shift of $E_F$ closer to the vHs. Comparisons are made to the core levels and valence bands of $Tl_2Ba_2CaCu_2O_{8+\delta}$ (Tl-2212) and $HgBa_2CaCu_2O_{6+\delta}$ (Hg-1212). The similarity of the $Cu 2p_{3/2}$ spectra for Tl-1212 and Tl-2212 indicates that the number of Tl-O layers has little effect on the Cu-O bonding. However, the Tl-1212 and Hg-1212 $Cu 2p_{3/2}$ signals exhibit differences which suggest that the replacement of $Tl^{+3}$ with $Hg^{+2}$ results in a decrease in the $O 2p \rightarrow Cu 3d$ charge transfer energy and differences in the probabilities of planar vs. apical oxygen charge transfer and/or Zhang-Rice singlet state formation on Cu sites away from the core hole. Differences between the Tl-1212 and the Tl-2212 and Hg-1212 measured valence bands are consistent with the calculated Cu 3d and (Tl, Hg) 6s/5d partial densities of states.

PACS Numbers: 74.72.Fq, 74.25.Jb, 74.76.Bz, 79.60.-i

# 1. introduction

Among the Tl cuprate high temperature superconductors, the $TlBa_2Ca_{n-1}Cu_nO_{3+2n-\delta}$ (Tl-12(n-1)n) family has received little attention relative to the Tl-22(n-1)n family, due to both the somewhat lower superconducting transition temperatures ($T_c$) and the greater difficulty in obtaining high quality Tl-12(n-1)n phases. Comparison of single and double "1'1-layer materials is of fundamental interest in determining the effect of the charge reservoirs and distance between Cu-O planes on the electronic structure. However, band structure calculations of single l'1-layer materials have been limited to a single tight binding study.[1]

Some interest in applications of the Tl-1223 phase has been motivated by its lower anisotropy, greater flux pinning and consequently higher critical current densities relative to the more commonly studied '1'1-2212 and "1'1-2223 phases. The 1'1-1212 phase also has greater flux pinning, but has been the subject of even fewer studies. The $T_c$ of 3'1-1212 depends sensitively on the oxygen doping,[2] varying in bulk powders from 80 K for samples synthesized in oxygen to as high as 110 K as $\delta$ increases, thus requiring controlled annealing in an inert atmosphere to achieve optimal doping by removal of excess oxygen. The growth of high quality epitaxial T]-1212 films, which are of interest for microwave device applications, has only recently been demonstrated.[3,4]

High temperature superconductors have been widely studied with photoemission spectroscopy. Valence band measurements provide a measure of the density of states, while core level measurements provide information on issues such as oxidation states and doping-induced chemical potential shifts and, in the case of the highly correlated Cu cations, charge transfer mechanisms and multiplet splitting. However, photoemission studies of the Tl cuprates have been limited by the difficulty in obtaining well-characterized, high quality materials, as well as by the well-known difficulty, common to all of the cuprates, in obtaining clean surfaces due to the reactivity of the alkaline earth components. Previous x-ray photoelectron spectroscopy (XPS) measurements on T]-1212 are limited to reports from a single groups''' The earlier XPS studies reported no detectable Fermi edge and were on polycrystalline samples scraped in vacuum,[5-7] which can yield surfaces with significant spectral contributions from nonsuperconducting grain

boundary species and/or artifacts from scrape-induced damage.[8] XPS measurements from higher quality Tl-1212 surfaces are therefore desirable.

in this work, XPS core level and valence band measurements are reported for high quality epitaxial Tl-1212 films. These results are compared to the band structure calculated in this work and to previously reported XPS measurements of Tl-1212 polycrystalline pellets.[5,7] The Tl-1212 film surfaces are demonstrated to be high quality, as shown by the relatively low intensities observed for the high binding energy contaminant signals in the O 1s and Ba core levels and the observation of a clear Fermi edge in the valence band region. Comparison of the data measured in this work to earlier measurements on epitaxial films of Hg-1212 (Ref. 9) and Tl-2212 (Ref. 1 O) yields information on the effects of varying the number of 'l'l-0 layers or replacing the $Tl^{+3}$ with $Hg^{+2}$. The effects of oxygen doping are investigated by comparing XPS spectra from as-grown and nitrogen-annealed Tl-1212 samples with significantly different $T_c$s. The eloping-induced core level shifts and change in $T_c$ are compared to expectations based on the band structure calculations, and the possible role of van Hove singularities is discussed. The measured Tl-1212 valence band density of states is compared to those of Tl-2212 and Hg-1212, and differences are explained by comparison of the calculated Cu 3d and (Tl,Hg) 6s/5d partial densities of states of these materials.

## 11. Experimental

Epitaxial 'l'l-1212 films on $LaAlO_3$ ( 100) substrates are obtained by sputter deposition of Tl-free precursor films followed by an *ex situ* anneal in a static two-zone furnace for thallination. Details of the. film growth, annealing, and characterization are described elsewhere.[4] Some of the films received an additional anneal in nitrogen at 250° C for one hour. Prior to the final nitrogen anneal, which adjusts the oxygen content, the films are typically superconducting at -70-75 K, while $T_c$ is raised to -85-90 K after nitrogen annealing.

The films were cleaned with a nonaqueous etchant consisting of 0.1 % $Br_2$ in absolute ethanol, rinsed in ethanol, and blown dry with nitrogen in the ultrahigh purity nitrogen atmosphere of a glove box which encloses the XPS load lock. This procedure minimizes exposure of the clean

surface to reactive atmospheric gases such as water vapor and carbon dioxide and has yielded high quality surfaces for other cuprate superconductors,[8] notably including the Tl cuprate phases "1'] -2212 (Ref. lo) and '1'1-2201 (Ref. 11) as well as the chemically and structurally similar Hg cuprate Hg-1212 (Ref. 9). The etch rate was found to be - 1000 Å/rein, and a 45s etch was sufficient for obtaining XPS spectra characteristic of high quality surfaces, using criteria described elsewhere.[8] The XPS spectra were accumulated on a Surface Science Spectra SSX-501 spectrometer with monochromatized Al $K_\alpha$ x-rays (1486.6 eV), photoemission normal to the film surface, and a base pressure of $5 \times 10^{-10}$ Torr. The x-ray beam diameter was 150 μm for the core level measurements and 300 μm for the valence band measurements. The pass energy of the electron energy analyzer was 25 eV, yielding a peak full width at half maximum (FWHM) of 0.7 eV for a Au $4f_{7/2}$ signal. The Fermi level of Au is taken to be the zero of binding energy, which yields a Au $4f_{7/2}$ binding energy, measured from a deposited Au film, Of 83.9 eV and a $Cu 2p_{3/2}$ binding energy, measured from an Ar ion-etched Cu plate, of 932.5 eV.

One fully oxygenated and two nitrogen-annealed films are measured in this work, and ac susceptibility measurements following the XPS measurements show a superconducting transition onset at 74.5 K with a transition width of 2 K for the oxygenated film, and superconducting transition onsets of 86 K and 87 K with transition widths of 1 K for the nitrogen-annealed film, Equivalent XPS spectra are obtained from both nitrogen annealed films, the spectra presented here are from the film with $T_c = 87$ K. The surface stoichiometries after etching for all three films measured in this work are near Tl:Ba:Ca:Cu = 1:1.85:1.15:2.

### 111. Band Structure Calculations

Since the oxygen content in Tl-O layers is of crucial importance for $T_c$, the electronic structure is calculated for "T1-1212 with two different oxygen contents; oric corresponds to $\delta = 0$ when all oxygen sites in the Tl-O layer tire occupied, and another corresponds to $\delta = 0.5$, when every other oxygen site is vacant.

To determine the electronic structure of "T1-1212, the full-potential linear muffin-tin orbital (FLMT)(l)" was used within the local density approximation (1 DA) and the Ceperly-Alder form of the exchange-correlation potential, In these calculations no shape approximations are made to either the charge density or the potential. The structural parameters for 'T1- 1212 are taken from Ref. 12. The unit cell consists of two Cu-$O_2$ layers (oxygen atoms in Cu-$O_2$ layers are referred to as 0(1)) separated by Ca, and a blocking layer containing Ba, "apical" oxygen (O(2)) and the T1-0 layer with its oxygen site referred to as 0(3). local atomic distortions around the oxygen vacancy site that were measured in Ref. 12 were taken into account in the calculations for 'T1-1212 ($\delta$=0.5).

The FLMTO calculations are performed in the spin-restricted scalar-relativistic mode with atomic $Ba(5s^25p^66s^26p^0)$, $Tl(5s^25p^65d^{10}6s^26p^1)$, $Cu(3s^23p^63d^{10}4s^1)$, $Ca(3s^23p^24s^2)$ and $O(2s^22p^4)$ levels treated as valence band electrons. A technique,[13] similar to Singh's "local orbitals",[14] is used to enable simultaneous treatment of orbit als with equal orbital number in the same energ y wi ndo w. 1( is well known that the LMTO scheme of band calculations works well for close-packed structures. in order to get a more close-packed structure, empty spheres are introduced at sites (0.5, 0.0, 0.0). The MT-radii are carefully chosen based on the spatial distribution of the self-consistent charge density over the unit cel].

The set of radii, $R_{Tl}$=2.0, $R_{Ba}$=3.4, $R_{ca}$= 2.84 and $R_O$=1.8 au., are used since these attribute charge densities centered at different atoms to their corresponding spheres, leaving only relatively smooth variations of the charge density over the interstitial region. A triple-kappa basis set is employed for each type of atom with angular momentum, $l$, up to 2 for Tl, Cu and O and up to 3 for Ba and Ca for $\kappa^2$=-0.01 Ry, and up to 1 for $\kappa^2$=- 1.() and -2.3 Ry. Wave functions with $l_{max}$=1 are associated with empty spheres for the first kappa value only. The charge density is calculated exactly in muffin-tin spheres for angular momentum components up to $l$=6. The same $l$ cut-off is used when interpolating in the interstitial region over f lankel functions with energies -1 and -3 R y. Calculations done for $l$=5 do not show any difference in band positions which indicates good convergence of the results with $l_{max}$.

The Brillouin-zone integrations arc carried out by the tetrahedron method using a 455 $k$-point mesh (corresponding to 12X12X 12 regular divisions along the $k_x$, $k_y$, and $k_z$ axes, respectively) in the 1/16 irreducible wedge.

Total and $l$-projected density 01 states (DOS) of "1'1-1212 ($\delta=$ O) are presented in Fig. 1 with the Fermi energy ($E_F$) chosen at O eV. The upper part of the valence band consists of strongly hybridized Cu 3d and O(1,2,3) 2p states. The effective width of the O 2p states decreases from O(1) to O(2) and O(3), reflecting a reduction 01 the covalent bonding of oxygen in different crystallographic positions. The part of the valence band located around - 10 CV consists mostly of Tl 5d and Ba 5p states with '1'1 5d states lying slightly above the Ba 5p. The states at -16 eV arc composed mainl y of O 2s states. A clear shift of the O 2s states for 0(1), O(2) and 0(3) suggests different degrees of ionization, being the least for oxygen in Tl-O layers. Another interesting feature is that 0(3) has a very narrow 2p band (compared to 0(1) and O(2)), which suggests that O(3) is incorporated in the structure as a loosely bonded ion. Thus, annealing in an inert atmosphere most probably affects onl y ox ygen i n Tl-O layers.

The band structure in the range from -18 eV to -t 5 eV relative to $E_F$ presented in Fig. 2 also shows three distinct groups of bands: in the upper energy arc Cu-O hybridized bands, Ba 5p - Tl 5d in the middle anti O 2s states at the bottom with a very flat band of O(3) 2s states.

Figure 3 presents the band structure in the vicinity of $E_F$ which looks very similar to the band structures of all layered Cu-O based high-"]', superconductors. Two :iltllc)st-lrcc-clcctrt)ll-like dpσ bands (their number corresponds to the number of Cu-O layers) cross the Fermi level. One can scc a prominent van 1 love singularity (vHs) which is located along the X-R direction in the BZ, as is usual for all tetragonal cuprate high-']', materials. [15]

q'eta] and I-decomposed DOS for '1'1-1212 ($\delta=0.5$) arc presented in Fig.4. The introduction of oxygen vacancies in the '1'1-0 layer produces quite dramatic changes in the band structure of 7'1-1212 (as compared to the $\delta=0$ case). First of all, the interaction strength of 0(3) with the rest of the crystal is changed: the 0(3) 2p band width is enlarged and shifts deeper below $E_F$ (cf. Fig.4), or alternatively $E_F$ shilts up in energy; the 0(3) 2s states arc now located in nearly the same energy

region as the O(1) 2s states, while the O(2) 2s states are shifted to approximately 2 eV below (higher binding energy than) the O(1) and O(3) 2s stares. This changes the O 2s state ordering found for the Tl-1212 ($\delta$=0) case. Also note that the Ba 5p states corresponding to the Ba atom with completely occupied 0(3) sites are 2 CV lower in energy (higher binding energy) than the 5p states of Ba with an 0(3) vacancy in its nearest vicinity. Such changes in oxygen and Ba states are caused by strong changes in the Madelung potential of the Tl-O layers induced by partial removal of the 0(3) atoms.

Another interesting feature of the Tl-1212 ($\delta$=0.5) electronic structure is the $E_F$ location, which lies well below the vI-Is in Tl-1212 ($\delta$=0), but in Tl-1212 ($\delta$=0.5) is in close proximity to the VHS. This is clearly seen in Fig.4, where $E_F$ is close to the DOS maximum produced by the vHs.


## IV. X1'S Core Level Measurements

The core level binding energies and peak FWHMs measured in this work from as-grown and nitrogen- annealed T1-1212 epitaxial films are sum marized in Table 1, together with measurements previously reported for 11-1212 polycrystalline pellets[5-7] and for Hg-1212 and T1-2212 epitaxial films.[9,10] The O 1s spectrum measured from a nitrogen-annealed Tl-1212 film after etching is compared in Fig. 5 to the corresponding spectra from 1lg-1212 and '1'1-2212 epitaxial films.[9,10] The peak near 531 eV, which is dominant prior to etching, is associated with contaminants,[8] particularly alkaline earth carbonates. The lower binding energy manifold is a minor component prior to etching and originates from the nonequivalent oxygen sites in the '1'1-1212 lattice. The dominance 01' the lower binding energy superconductor signals in Fig. 5 demonstrates the surface cleanliness obtained in this work. in contrast, earlier studies of polycrystalline Tl cuprates[5-7] exhibited O 1s spectra with contaminant and superconductor signals nearly equal in intensity.[c]

The Tl-1212 O 1s signal consists of two components, as demonstrated more clearl] y in the second derivatives of the spectra shown in the inset 01' Fig. 5. As previously mentioned, O(3) in the Tl-O planes is the oxygen with the. lowest binding energy for $\delta$ = 0, and has nearly the same

binding energy as the 0( 1 ) states for $\delta \doteq 0.5$. Assuming 75% O(3) occupancy for optimal] y doped Tl-1212,[12] the 0(3) signal would account for only 11% of the total O 1s intensity, and would be <20% of the intensity of the 0(1) signal from Cu-O planes. The lowest binding energy signal whit.b is resolvable in Fig. 5 is the signal with the greatest intensity, and is therefore assigned to Cu-O planes, consistent with studies of other cuprate superconducto rs.[9,10,16-21] The higher binding energy component is assigned to "1'1-0(2) bonding, consistent with the O state ordering found in the band structure calculations in this work and with previous experimental assignments.[10,16,19,21] The 0(3) signal would either contribute to the O(1) signal or would be an unresolvabl y small component on the low binding energ y side of the much more intense 0(1) signal. These assignments are verified with angle-resolved measurements, which show that at a photoelectron emission angle $70°$ from normal the '1'1, Ba, and higher binding energy O 1s core level signals are enhanced relative to the Cu and lower binding energy O 1s core level signals. These observations suggest 1'1-0 surface termination, consistent with previously reported measurements of chemically etched Tl-2212.[21] The relative Ca abundance is not angle-dependent, which likely results from Ca occupying multiple lattice sites, as discussed later.

The O 1s signals of Tl-22 2 and Ilg-1212 also consist of two components, as shown for comparison in the inset of Fig. 5, with the high binding energy component of Ilg-1212 being associated with Hg-O bonding. The two O 1s components have the same binding energies for llg-1212 and '1"1-22 12, with different intensity ratios yielding the observed difference in the manifold lineshapes. For Tl- 1212 and llg-1212, on the other hand, the difference in observed manifold lineshapes originates from two O 1s components having similar intensities but differing binding energies, with the energy separation being 0.3-0.4 eV less for 3'1-1212.

The T] 4f and Ba 4d spectra are presented in Fig. 6. Least squares fitting shows that the Tl 4f spectrum is consistent with a single doublet, in agreement with previous measurements from '1'1-12 12 polycrystalline pellets scraped in vacuum,[5-7] as well as other T] cuprates. [9,16,19,22,23] The Tl $4f_{7/2}$ binding energy, which in '1"1 cuprates is intermediate between $Tl_2O$ and "1'1$_2${}$_3$, has been interpreted[5-7,23] as evidence that "1'1 is in an intermediate oxidation state between +1 and +3, being

nearly +3 for T1-1212. Similarly, the increase in the Tl $4f_{7/2}$ binding energy with decreased hole doping when $Y^{+3}$ is substituted for $Ca^{+2}$ has been interpreted[7] as a change in the Tl valence. However, in this work the primary effect of a change in the doping level is found to be a shift of the Fermi level, as discussed later.

The Ba 4d (Fig. 6) and 3d (not shown) spectra consist of the dominant superconductor signal, and a lower intensity contaminant signal at higher binding energy. An earlier study[6] of Tl-1212 found a $Ba\, 3d_{5/2}$ binding energy 0.7 eV higher than that measured in this work. However, the O 1s signal exhibits a significantly higher contaminant signal in the earlier work[6] compared to this work, and the Ba 3d signal, with lower photoelectron kinetic energy, is more surface sensitive. Since the energy separation of the Ba 3d signals from the superconductor and contaminants is nearly the same as the peak width, the lower binding energy observed in this work reflects the lower level of contaminants. The band structure results in Fig. 4 suggest that Ba atoms near O(3) vacancies should yield photoemission signals at -2 eV lower binding energy than Ba atoms near occupied O(3) sites. Assuming 75% O(3) occupancy, the Ba signal should therefore consist of two signals with a 3:1 ratio between the high and low binding energy components, which is not observed in Fig. 6. Some possible reasons for this apparent discrepancy are that the splitting of the states may be more pronounced for the shallow Ba 5p core levels, the band structure calculated for $\delta = 0.5$ may not be directly comparable to a doping level of $\delta = 0.25$, or the crystal structure determined for $\delta = 0.25$ may not be completely accurate for the calculations of the $\delta = 0$, 0.5 cases.

The Ca 2p spectrum in Fig. 7 consists of two doublets, as shown in the least squares fitting results in Fig. 7, both of which are associated with Tl-1212. Prior to etching, a higher binding energy surface contaminant signal with a $Ca\, 2p_{3/2}$ component near 347 eV is also prominent, but is not detectable after etching. The two doublets evident in Fig. 7 are also observed in the Ca 2p spectra of Hg-1212 (Ref. 9) and Tl-2212 (Ref. 10), as well as other Ca-containing cuprates such as $Bi_2Sr_2CaCu_2O_{8+\delta}$ (Di-2212),?() and have been interpreted as originating from occupation of inequivalent lattice sites due to cation disorder, with the lower binding energy doublet assigned to

the site between Cu-O planes. As in other alkaline earth compounds in general and cuprate superconductors in particular, the Ba and Ca core level binding energies of Tl-1212 measured in this work are significantly lower than those of the corresponding metals, which has been attributed to initial state electrostatic effects, specifically the Madelung energy being larger than the ionization energy.[24 27]

The Cu $2p_{3/2}$ spectra measured from Hg-1212, T1-1212, and Tl-2212 are compared in Fig. 8, and are typical Of $Cu^{+2}$ compounds. The satellite at higher binding energy corresponds to a multiplet of $\underline{2p}^5 3d^9 \underline{L}$ states, where underscoring denotes a hole and 1. denotes the oxygen ligand, and the main peak near 933 CV is usually attributed to well-screened $\underline{2p}^5 3d^{10}\underline{L}$ final states resulting from ligand-to-metal (O 2p → Cu 3d) charge transfer.[28,30] The relatively large width (> 3 cV) and asymmetry of the 933 CV signal cannot be explained by core. hole lifetime broadening or instrumental resolution, or by multiplet splitting, which would not be expected when the Cu 3d states are fully occupied, and are usually attributed to O 2p band effects. The main peak binding energy and width and the satellite/main peak intensity ratio, $I_s/I_m$, for '1"1-1212 measured in this work are in general agreement with those reported for' Tl-1212 polycrystalline pellets scraped in vacuum.[6,7] The satellite - main peak energy separation and $I_s/I_m$ are related to the O 2p - Cu 3d hybridization and charge transfer energy;[29,30] the similarity of the Cu $2p_{3/2}$ spectra for 1"1-1212 and '1'1-2212 (see Fig. 8 and Table 1) thus indicates that the number of Tl-O layers has little effect on the Cu-O bonding. However, the T]-1212. and Hg-1212 Cu $2p_{3/2}$ signals do differ, with the Hg-1212 signal having a lower value of $I_s/I_m$ and the main signs] being broader on the low binding energy side. Such observations could be an indication of oxygen deficiency in the }lg-1212, which would be accompanied by an increased intensity on the high binding energy side of the O 1s signal (near 52,9 cV, e.g. see Refs. 21, 3 1). This possibility can be eliminated by examination of Fig. 5, which shows that the Hg-1212 O 1s signal has enhanced intensity at lower binding energy compared to the 'T1- 1212 signal. The observed differences in the "1'1-1212 and Hg-1212 Cu $2p_{3/2}$ signals thus appear to be intrinsic. The lower value of $I_s/I_m$ observed for Hg-1212 indicates that replacement of $Tl^{+3}$ with $Hg^{+2}$ results in a lowering Of the O 2p → Cu 3d charge transfer energy. The observed

differences in the $Cu\,2p_{3/2}$ main peak widths, according to the conventional interpretation, should reflect differences in the O 2p bandwidths. However, the calculated O 2p bandwidth for 1lg-1212 (Ref. 32) dots not differ significantly from that for '1'1-1212 (see Fig. 1), so other possibilities must be considered.

Two models have recently been proposed which result in the $Cu\,2p_{3/2}$ main peak having contributions from more than one final state. In one model, the $Cu\,2p_{3/2}$ main peak consists of two final states corresponding to charge transfer from Cu-O plane oxygens (O $2p_{x,y} \rightarrow Cu\,3d_{x^2-y^2}$) and apical oxygens (O $2p_z \rightarrow Cu\,3d_{z^2}$).[33] This model is consistent with the larger $Cu\,2p_{3/2}$ main peak widths and asymmetric lineshapes (skewed towards higher binding energy) observed from Cu compounds with pyramidal or octahedral oxygen coordination compared to compounds with square planar oxygen coordination. However, 1'1-1212 and IIg-1212 are isostructural, with Cu having pyramidal oxygen coordination in both compounds. 11 this model is correct, then the observed Iineshape differences may reflect differences in the planar vs. apical oxygen charge transfer probabilities. In the second model, the $Cu\,2p_{3/2}$ main peak consists of $\underline{2p^5 3d^{10}\underline{L}}$ final states at higher binding energy, and lower binding energy $\underline{2p^5 3d^{10}}$ final states which result from core hole repulsion yielding Zhang-Rice singlet states on neighboring Cu sites.[34] If this model is correct, then the observed lineshape differences may reflect differences in the probability y of Zhang-Rice singlet state formation on Cu sites away from the core hole. Both mechanisms may contribute to the $Cu\,2p_{3/2}$ main peak width anti complex lineshape.

## V. Effect of Doping on the Chemical Potential

"1'1-1212 is unusual in that even for a stoichiometric oxygen content ($\delta = 0$), the Fermi level lies below the vI Is seen so prominently in Fig. 3 at the R point ($E_F$ typically lies above the vI Is and hole doping is required to lower it onto the VI 1s). in several models,[35] the VI 1s is regarded as one of the main reasons for high $T_c$ superconductivity. However, the recent observat i ons of an extended VI Is near the Fermi level for Bi-2201($T_c$ -10 K)[36] and $Sr_2RuO_4$ ($Tc$ -1 K)[37,38] suggest that the VI Is may be necessary but not sufficient for producing high '1', superconductivity. Even

though the vHs may not be directly responsible for high $T_c$ superconductivity, the role of the vHs in those compounds which do exhibit high $T_c$ superconductivity appears to be that an optimum $T_c$ is associated with an $E_F$ shifted onto or close to the vHs. Thus, the fact that $E_F$ crosses the X-R line of the vHs makes it understandable why samples of Tl-1212 synthesized in oxygen are already high $T_c$ superconductors. In order to increase $T_c$ further, $E_F$ must shift upwards onto the prominent vHs at the R-point.

The core levels measured in this work from both nitrogen-annealed Tl- 1212 films are consistently observed at slightly higher binding energies than those of the as-grown sample (see 'Table 1). With the exception of the $Cu 2p_{3/2}$ signal, for which the width of the signal makes detection of small shifts difficult, these binding energy shifts ($\pm 0.05$ eV) are in the range 0.04 - 0. 11 eV for the $T_c = 87$ K sample, and 0.04 -0.17 eV for the $T_c = 86$ K sample. The higher values may be more reliable, since the lower values are from the Ca 2p and O 1s signals, which consist of overlapping components whose binding energies determined from least squares fitting may have greater uncertainty. Core potential differences due to changes in effective charges, or to changes in the Madelung potential (c. g. from bond length changes) would be expected to have opposite effects on different sites. The observed shifts in the core level binding energies in the same direction by nearly the same amount (within experimental error) with doping thus suggests that the change in the chemical potential is the dominant effect of doping. Doping-induced changes in chemical potentials have previously been reported for 'Tl-2201 ,[16] as well as for other cuprates.[39-43]

During the process of annealing in nitrogen, oxygen is depleted from the 0(3) position (since, as indicated above, it is the weakest bonded ion) and so add electrons to the conduction band. As shown by the "Tl-1212 ($\delta = 0.5$) calculations, this shifts $E_F$ onto the vHs at the R-point. The observations that $T_c$ increases and the core levels shift to higher binding energies with nitrogen annealing are consistent with a reduction in the level of hole doping and a shift of $E_F$ close to the vHs that are expected with the removal of oxygen. Clearly, in this view, the same effect could also be achieved through trivalent ion substitutions for Ca. in fact, substitution of Nd, Gd, or Y for Ca

in '1'1-1212 has been reported to increase 'T$_c$, with maximum T$_c$ occurring for 30% substitution,[44] and substitution of Y for Ca has been reported to result in an increased Tl 4f$_{7/2}$ binding energy.' In the latter study, the increased Tl 4f$_{7/2}$ binding energ y was interpreted as evidence for a change in the Tl valence, rather than a change in the chemical potential, since the Cu2p$_{3/2}$ binding energy was not doping dependent. It is difficult to assess the validity of this interpretation since other core level measurements were not reported. However, the possibility that a Fermi level shift could have been masked is suggested by the higher levels of surface contaminants in the earlier studies[5-7] and the greater surface sensitivity and large width of the Cu2p$_{3/2}$ signal.

## VI. X1'S Valence Band Measurements

Fig. 9 compares the valence bands and the Tl 5d and Ba 5p shallow core levels of Tl- 1212 and T1-221 2, scaled to facilitate comparison of line shape differences in the valence band region. The Fermi edges, not reported in earlier studies of Tl- 12. 12,[5-7] are shown more clearly in the inset, further demonstrating the surface quality. The valence bands consist primarily of Cu 3d, O 2p, and "1'1 6s/5d states, with the Cu and Tl states contributing most of the spectral weight for the photon energy used in this work.[45] Distinct differences in the measured '1'1-1212 and Tl-22 12 1)0S are apparent in Fig. 9. The shoulder near 7 CV in the '1'1-2212 spectrum consists primarily of 11 6s States.[45,46] This feature is less prominent in the "T1-1212 spectrum, reflecting both the smaller Tl/Cu ratio relative to 1'1-2212 and the occurrence of the "1'1 6s states at lower binding energ y, near 5 CV (sec Fig.1). TI-2212 also exhibits significant Tl 6s/5d spectral weight throughout the energy range 3-7 cV,[45] so that the larger Tl/Cu ratio relative to Tl- 1212 is consistent with the larger observed intensity at greater than 4 CV binding energy. However, the T]-1212 valence band shape is more skewed towards high binding energy despite the lower Tl partial DOS in this region. Below the valence bands in Fig. 9 are the Cu 3d partial DOS (the primary contributions to the measured valence bands) from band structure calculations of T]-1212 (top, this work) and 'H-2212 (bottom, Ref. 46), shifted by 2 eV to approximately match the envelopes of the valence bands. Electron correlation effects have often been cited as necessitating similar shifts for other cuprate

superconductors. The skewing of the T]-1212 valence band towards higher binding energy may be a reflection of the more sharply peaked Cu3d partial DOS in the region 5-6 cV.

The valence bands and shallow core levels of T1-1212 and Hg- 12 12 are compared in Fig. 1 0. 3-he most striking difference in the valence bands is the increased intensity near 5 CV in the Hg-121 2 spectrum. The Hg-1212 Cu3d partial DOS is similar to that of "1'1-2212 (scc the comparison in Ref. 9), and the differences with T]-1212 are not sufficient to account for the observed spectra. Shown below the valence bands in Fig. 10 are the Hg-1212 Hg 5d (top, Ref. 32) and Tl- 12121'1 5d (bottom, this work) partial DOS in the energy range of interest. The occurrence of' Hg 5d states near 5 CV for Hg-1212 and the. lack of corresponding states for Tl-1212 are. consistent with the observed differences in the measured valence bands.

## VII. Summary & Conclusions

The core levels of high quality 1'1-1212 epitaxial films were measured with XPS, and the valence electronic structure was determined by band structure calculations and measured with XPS. The surface quality has been demonstrated by the low level of high binding energy signals from contaminants in the O 1s and alkaline earth core level regions, and by the observation of a Fermi edge in the valence band region. The "1"1-1212 oxygen 1s signal is resolved into two components, associated with Cu-O planes and Tl-O bonding. The similarity of the '1'1- 1212 and '1'1-2212 Cu $2p_{3/2}$ spectra shows that the number of Tl-O layers has little effect on the Cu-O bonding. However, the "1'1-1212 and Hg-12 12 Cu $2p_{3/2}$ signals exhibit differences which suggest that the replacement of $Tl^{+3}$ with $Hg^{+2}$ results in a decrease in the O 2p $\rightarrow$ Cu 3d charge transfer energy, as wc] l as di fferences in t he probabilities of planar vs. apical ox ygen charge transfer and/or Zhang-Rice singlet state formation on Cu sites away from the core hole. Measurements from samples with differing $T_c$s resulting from differing oxygen doping levels show that, within experimental error, the core levels are rigidly shifted, consistent with a doping-induced change in chemical potential. The band structure calculations show that for the stoichiometric compound ($\delta$=0) the van Hove singularity is above $E_F$, and is close to $E_F$ for $\delta = 0.5$. Samples annealed in nitrogen (to

reduce the hole overdoping by the removal of oxygen) exhibit higher core level binding energies and hi gher $T_c$, consistent with a shift of $E_F$ onto or nearer the vI Is. Differences between the valence bands of 'I'J-1212 measured in this work and previous] y measured 'I''1-2212 and 1lg-1212 valence bands arc consistent with differences in the calculated Cu 3d and (Tl, Hg) 6s/5d partial DOS.

## Acknowledgements

# References

1. S. V. Meshkov, S. N. Molotkov, S. S. Nazin, I. S. Smirnova, and V. V. Tatarskii, Physics C 166, 476 (1990).

2. S. Nakajima, M. Kikuchi, Y. Syono, K. Nagase, 1. Oku, N. Kobayashi, D. Shindo, and K. Hiraga, Physics C 170, 443 (1990).

3. M. P. Siegal, N. Missert, E. 1,. Venturini, P. P. Newcomer, F. Dominguez, and R. Dunn, IEEE Trans. Appl. Supercond. S, 1343 (1995).

4. M. P. Siegal, E. L. Venturini, P. P. Newcomer, B. Morosin, D. 1.. Overmyer, F. Dominguez, and R. Dunn, Appl. Phys. Lett. 67, 3966 (1 995).

5. T. Suzuki, M. Nagoshi, Y. Fukuda, S. Nakajima, M. Kikuchi, Y. Syono, and M. Tachiki, Physics C 162-164, 1387 (1 989).

6. Y. Fukuda, T. Suzuki, and M. Nagoshi, i n *Thallium-Based High Temperature Superconductors, Eels.* A. M. Hermann ant] J. V. Yakhmi (Marcel Dekker, inc., New York, 1994), Chapter 24, pp. 511-522.

7. T. Suzuki, M. Nagoshi, Y. Fukuda, S. Nakajima, M. Kikuchi, Y. Syono, and M. Tachiki, Supercond. Sci. Technol. 7, 817 (1 994).

8. R. P. Vasquez, J. Electron Spectrosc. Relat. Phenom. 66, 209 ( 1994), and references [herein.

9. R. P. Vasquez, M. Rupp, A. Gupta, and C. C. Tsuei, Phys. Rev. B 51, 15657 ( 1995).

lo. R. P. Vasquez and W. L. Olson, Physica C 177, 223 (1991).

11. B. Morosin, D. S. Ginley, P. F. Hlava, M. J. Carr, R. J. Baughman J. E. Schirber, E. L. Venturini, J. F. Kwak, Physics C 1S2, 413 (1988).

12. M. Methfessel, Phys. Rev. B **38**, 1537 (1988).

13. M. Schilfgaarde, unpublished.

14. 1). Singh, "Plane waves, pseudopotentials and the LAPW method", Kluwer Academic Publ., 1994; D. Singh, Phys. Rev. B 43, 6388 (1991).

15. D.1.. Novikov, A. J. Freeman, Lecture Note.s in Physics, Springer-Verlag, to be published.

16. R. P. Vasquez, Z. F. Ren, and J. H. Wang, Phys. Rev. B 54, 6115 (1996).

17. J. 11. Weaver, H. M. Meyer 111, T. J. Wagener, D. M. Hill, Y. Gao, 1.). Peterson, Z. Fisk, and A, J. Arko, Phys. Rev. B 38, 4668 (1988).

18. H. M. Meyer 111, D. M. Hill, J. H. Weaver, D.1.. Nelson, and C. F. Gallo, Phys. Rev. B 38, 7144 (1988).

19. H. M. Meyer 111, T. J. Wagener, J. H. Weaver, and D. S. Ginley, Phys. Rev. B 39, 7343 (1989).

20. F. Parmigiani, Z. X. Shen, D. B. Mitzi, I. Lindau, W. E. Spicer, and A. Kapitulnick, Phys. Rev. B 43, 3085 (1991).

21 R. P. Vasquez, B. D. Hunt, M. C. Foote, L. J. Bajuk, and W. L. Olson, Physics C 190, 249 (1992).

22. A. E. Bocquet, J. F. Dobson, P. C. Healey, S. Myrha, and. J. G. Tlhompson, Phys. Stat. Sol. (b) 152, 519 (1989).

23. T. Suzuki, M. Nagoshi, Y. Fukuda, Y. Syono, M. Kikuchi, N. Kobayashi, and M. Tachiki, Phys. Rev. B 40, 5184 (1989).

24. R. P. Vasquez, J. Electron Spectrosc. Relat. Phenom. 56, 217 (1 991).

25. C. Sousa, T. Minerva, G. Pacchioni, P. S. Bagus, and F. Parmigiani, J. Electron Spectrosc. Relat. Phenom. 63, 189 ( 1993).

26 R. P. Vasquez, J. Electron Spectrosc. Relat. Phenom. 66, 241 ( 1994), and references therein.

27. M. Nagoshi, Y. Syono, M. Tachiki, and Y. Fukuda, Phys. Rev. B 51, 9352 ( 1995).

28. S. 1 ,arsson, Chem. Phys. Lett. 40, 362 ( 1976).

29. G. van der Laan, C. Westra, C. Haas, and G. A. Sawatzky, Phys. Rev. B 23, 4369 (1981).

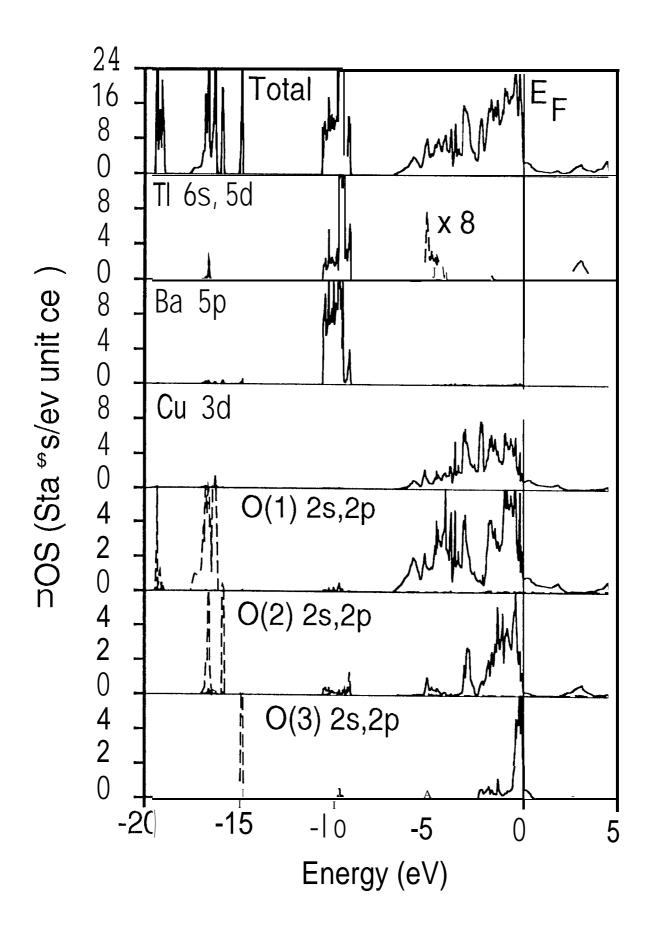30. F. Parmigiani and L. Sangaletti, J. Electron Spectrosc. Relat. Phenom. 66, 223 (1994), and references therein.

31    R. P. Vasquez, M . C. Foote, L. Bajuk, and B. D. Hunt, J. Electron Spectrosc. Relat. Phenom. **57,** 317 **(1991).**

32.   1>. 1,. Novikov and A. J. Freeman, Physica C **216,** 273 (1993).

33.   F. Parmigiani, L. E. Depero, 1'. Minerva, and J. B. Torrance, J. Electron Spectrosc. Relat. Phenom. 58, 315 (1992).

34.   M. A. van Veenendaal, H. Eskes, and G. A. Sawatzky, Phys. Rev. B 47, 11462 (1 993).

**35.**   R. S. Markiewicz, Physics C 217, 381 (1993).

**36.**   D. M. King, Z.-X. Shen, D. S. Dessau, D. S. Marshal], C. H. Pink, W. E. Spicer, J. L. Peng, Z. Y. Ii, and R. I. Greene, Phys. Rev. Lett. **73, 3298 (1994).**

37    1'. Yokoya, A. Chainani, T. Takahashi, H. Katayama-Yoshida, M. Kasai, and Y. Tokura, Phys. Rev. Lett. 76, 3009 (1996).

38.   11.11. I .u, M. Schmidt, '1'. R. Cummins, S. Schuppler, F. Lichtenberg, and J. G. Bednorz, Phys. Rev. Lett. 76, 4845 (1996).

39.   Z.-X. Shen, D. S. Dessau, B. O. Wells, C. G. Olson, D. B. Mitzi, L. Lombardo, R. S. List, and R. J. Arko, Phys. Rev. B 44, 12098 (1991).

40.   M. A. van Veenendaal, R. Schlatmann, G. A. Sawatzky, and W. A. Groen, Phys. Rev. B 47, 446 (1993).

41.   M. A. van Veenendaal, G. A. Sawatzky, and W. A. Groen, Phys. Rev. B 49, 1407 ( 1994).

42.   G. Rietveld, M. Glastra, and D. van der Marel, Physics C 241, 257 (1 995).

43.   G. Rietveld, S. J. Collocott, R. Driver, and D. van der Marel, Physics C 241, 273 ( 1995).

44.   S. Nakajima, M. Kikuchi, Y. Syono, N. Kobayashi, and Y. Mute, Physics C 168, 57 (1989).

45    P. Marksteiner, J. Yu, S. Massidda, A. J. Freeman, J. Redinger, and P. Weinberger, Phys. Rev. B **39,** 2894 (1989).

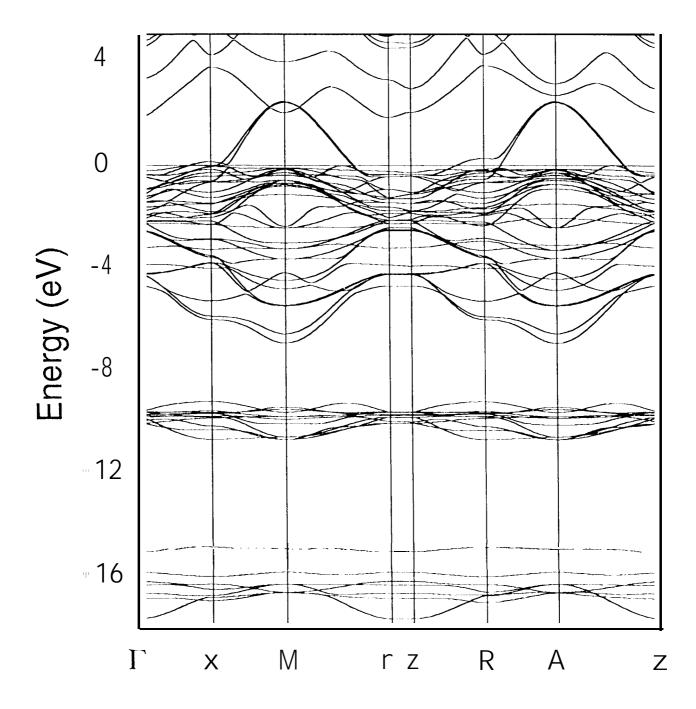46.   J. Yu, S. Massidda, and A. J. Freeman, Physica C 152, 273 (1988).

Table I. Summary of core level binding energies (±0.05 eV), peak full widths at half maximum (in parentheses), and Cu $2p_{3/2}$ satellite to main peak ($I_s/I_m$) intensity ratios (±0.02) for Tl-1212 epitaxial films measured in this work, together with previously reported results for Tl-1212 polycrystalline pellets and for Tl-2212 and Hg-1212 epitaxial films.

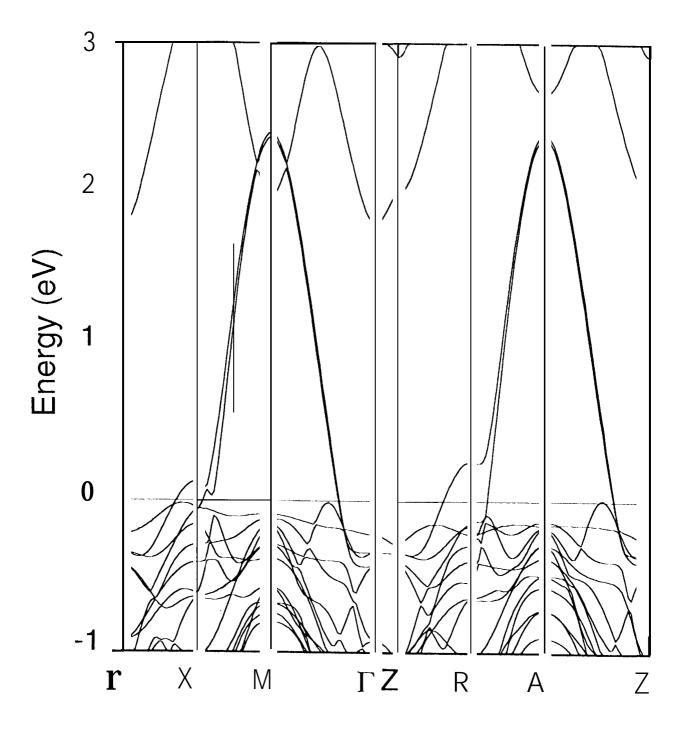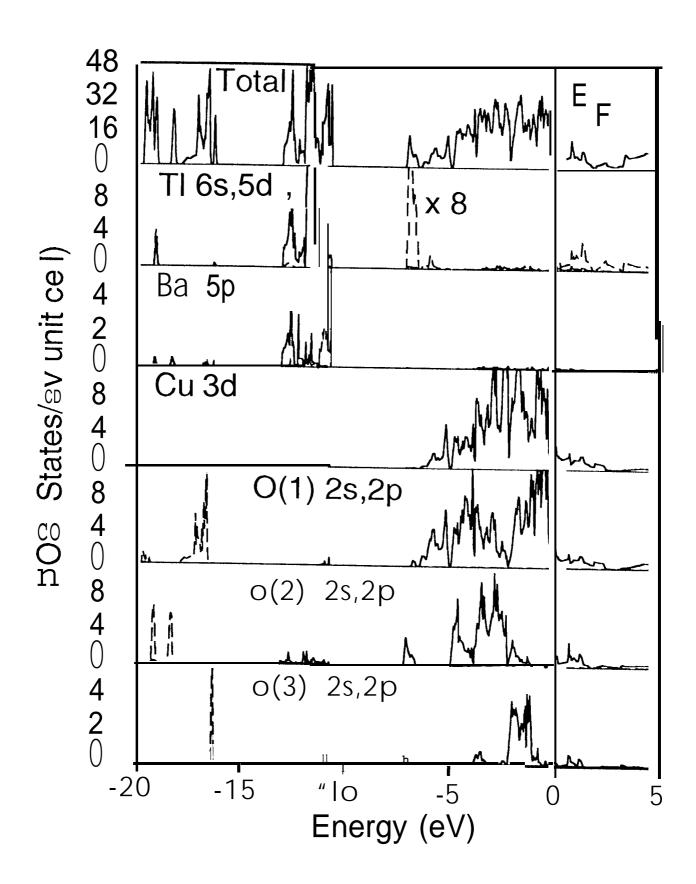| Material | Tl $4f_{7/2}$ | Ba $3d_{5/2}$ | Ba $4d_{5/2}$ | Ca $2p_{3/2}$ | Cu $2p_{3/2}$ | $I_s/I_m$ | O 1s | Ref. |
|---|---|---|---|---|---|---|---|---|
| Tl-1212 ($T_c$ = S7 K) | 117.75 (1.4) | 778.09 (1.4) | 87.67 (1.15) | 344.61 (1.2) & 345.68 (1.2) | 933.1 (3.2) | 0.44 | 527.99 (1.0) & 528.64 (1.2) | This work |
| ($T_c$ = 86 K) | 117.S3 (1.4) | 778.13 (1.5) | 87.71 (1.15) | 344.61 (1.3) & 345.70 (1.4) | 933.1 (3.3) | 0.42 | 528.02 (1.0) & 528.72 (1.1) | This work |
| ($T_c$ = 74.5 K) | 117.66 (1.4) | 777.99 (1 .5) | 87.56 (1.2) | 344.57 (1.2) & 345.60 (1.2) | 933. 1 (3.2) | 0.43 | 527.93 (1.0) & 528.60 (0.9) | This work |
| ($T_c$ = 73-79 K) | 117.7 (1.5) | 778.8 | not reported | 345.0 | 933.3 (3.4) | 0.41 | ~529 | 5-7 |
| Tl-2212 ($T_c$ = 102 K) | 118.02 (1.25) | 778.27 (1.55) | 87.87 (1.15) | 344.66 (1.2) & 345.73 (1 .2) | 933.1 (3.1) | 0.45 | 527.84 (0.9) & 528.69 (1.4) | 10 |
| Hg-1212 ($T_c$ = 117 K) | none | 778.21 (1.45) | 87.83 (1.1) | 344.48 (1.1) & 345.62 (1.2) | 932.9 (3.4) | 0.36 | 527.87 (0.9) & 528.72 (1.1) | 9 |

# Figure Captions

1. Total and *l*-projected DOS for T1-1212 ($\delta=0$). 'T'1 6s and O 2s DOS are shown by dashed lines. The scale for the Tl 6S states are enlarged by a factor of 8.

2. FLMTO band structure along high-symmetry directions for T]-1212 ($\delta=0$).

3. FLMTO band structure in the Fermi energy region for1"1-1212 ($\delta=0$).

4. Total and *l*-projected DOS forT1-1212 ($\delta=0.5$). 'T'1 6s, Ba (near the 0(3) vacancy) 5p and O 2s DOS are shown by dashed lines. The ']'] 6s states are shown enlarged by a factor of 8.

5. The O 1s spectra measured from chemically-ctched epitaxial films of 'T'1- 1212 (this work), ~"1-2212 (Ref. 10), and Jlg-1212 (Ref. 9). The inset shows the second derivatives of the spectra.

6. The Tl 4f and Ba 4d spectra measured for Tl- 1212, together with the results of least-squares fitting.

7. The Ca 2p spectrum measured for1"1-1212, together with the results of least-squares fitting.

8. The Cu $2p_{3/2}$ spectra measured for 1'1-1212 (this work), T1-2212 (Ref. lo), and IIg-1212 (Ref. 9).

9. The valence bands and the Tl 5d/Ba 5p shallow core level spectra measured from 1']-1212 (this work) and 1'1-2212 (Ref. 10). The inset shows the Fermi edges. Below the valence bands are the calculated Cu 3d partial densities of states of Tl-1212 (top, this work) and T1-2212 (bottom, from Ref. 46).

1(). The valence bands and shallow core levels measured for '1'1-1212 (this work) and IIg-1212 (Ref. 9). The inset shows the Fermi edges. Below the valence bands are the calculated "T1-1212127'1 5d (bottom, this work) and Jlg-1212 IIg 5d (bottom, from Ref. 32) partial densities of states in the binding energy range 2-7 cV.

INTENSITY (arbitrary units)

BINDING ENERGY (eV)

535    530    525

d²I(E)/dE²

530    E (eV)    525

Hg-O
Tℓ-O
Cu-O

O 1s
—— Tℓ-1212
- - Hg-1212
—— Tℓ-2212

Cu 2p$_{3/2}$

$\underline{2p}^5d^{10}\underline{L}$

$\underline{2p}^5d^9\underline{L}$

Hg-1212

T$\ell$-1212

T$\ell$-2212

INTENSITY (arbitrary units)

945    940    935    930

BINDING ENERGY (eV)